



ELSEVIER

27 March 1995

PHYSICS LETTERS A

Physics Letters A 199 (1995) 249–256

Dimensional crossover in organic networks

Nguyen Ba An¹, Eiichi Hanamura*Department of Applied Physics, University of Tokyo, 7-3-1 Hongo, Bunkyo-ku, Tokyo 113, Japan*

Received 6 January 1995; revised manuscript received 12 January 1995; accepted for publication 12 January 1995

Communicated by V.M. Agranovich

Abstract

Simple but precise expressions of exciton dipolar interaction are derived as a function of lattice constants and orientations of transition dipole moment and wavevector. Angle-dependent dimensional crossovers are studied in the long wavelength limit. A brief discussion is also given on optical responses associated with the crossover effect.

1. Introduction

Modern techniques of crystal growth have made available high quality low dimensional quantum structures of inorganic materials, such as semiconductor quantum wells, wires and dots. Any dimensional crystals of J-aggregates of dyes have been successfully grown by using the Langmuir–Blodgett method [1]. Molecular crystalline-like thin films and multilayers have recently been prepared [2,3] and investigations on such organic systems have just started (see, e.g., Refs. [4–7]). Phenomena at the interface between organic and inorganic quantum wells have also become a topic of research [8]. Unlike inorganic heterostructures, the organic molecular crystals, which are held together by weak van der Waals forces, may have large differences in the lattice constants in three dimensions. This allows one to prepare organic heterostructures of distinct dimension by choosing suitable lattice constant ratios. For example, depending upon the relative lattice constants, a bulk network of $[\text{PbI}_6]^{4-}$ octahedra may be treated as zero-dimensional (0D)

(e.g., $(\text{CH}_3\text{NH}_3)_4\text{PbI}_6 \cdot 2\text{H}_2\text{O}$), two-dimensional (2D) ($(\text{C}_n\text{H}_{2n+1}\text{NH}_3)_2\text{PbX}_4$; X = I, Br, Cl) or three-dimensional (3D) (e.g., $(\text{CH}_3\text{NH}_3)\text{PbI}_3$) systems. In synthesizing molecular crystals, one may have a family of structures with different lattice constants in three dimensions, which will cause a dimensional crossover effect within the same family. Moreover, dimensional crossovers are subject to the polarization configuration. Therefore, a study of direction-dependent dimensional change as a function of lattice constant ratio proves to be of real necessity and gains its own interest in many aspects. Optical responses of organic networks are governed by Frenkel excitons which propagate from one molecule to others by dipole–dipole interaction. Excitonic structures and their optical responses are almost determined by this dipole–dipole interaction. In the present Letter, the dimensional effect and dimensional crossover of Frenkel excitons are studied in the long wavelength limit in connection with its significance in specific physical applications. We also briefly discuss the effects of the dimensional crossover on optical responses. These crossover effects of dipole–dipole interaction concern not only Frenkel excitons but also

¹ Permanent address: Institute of Physics, P.O. Box 429 Bo Ho, Hanoi 10000, Vietnam.

magnons in magnetic systems and optical phonons of lattice vibrations.

2. Dipolar interaction

Consider an organic structure of the Bravais type with basic lattice vectors \mathbf{a}_1 , \mathbf{a}_2 and \mathbf{a}_3 , which are along the x , y and z axis, respectively (generalization to the case of nonorthogonal lattices is tedious but straightforward). The exciton dipolar interaction in this structure is given in the form

$$D^{\mu}(\mathbf{k}; a_1, a_2, a_3) = \sum_{\alpha\beta} \mu_{\alpha}\mu_{\beta} D_{\alpha\beta}(\mathbf{k}; a_1, a_2, a_3),$$

$$\alpha, \beta = 1(x), 2(y), 3(z), \quad (1)$$

$$D_{\alpha\beta} = \sum_{\{n_i\}}' \frac{e^{2\pi i \mathbf{k} \cdot \mathbf{r}}}{r^3} \left(\delta_{\alpha\beta} - \frac{3r_{\alpha}r_{\beta}}{r^2} \right). \quad (2)$$

Here $\mathbf{r} = n_1\mathbf{a}_1 + n_2\mathbf{a}_2 + n_3\mathbf{a}_3$, $r_{\alpha} = n_{\alpha}a_{\alpha}$. The prime excludes the term with $\{n_i\} \equiv 0$ and \mathbf{k} is the exciton propagation wavevector. We restrict ourselves to the electronic transition within a lattice cell from its s-like state to a triply degenerate p-like excited state. Then the point-like transition dipole moment $\boldsymbol{\mu}$ consists of three independent vectors $\boldsymbol{\mu}^P$ ($P = \text{I, II, III}$). Evaluation of the dipole lattice sums is an old [9–15] but still attractive [16] problem. These sums converge very slowly and commonly accepted procedures [9,10,12] use generalized theta functions and their transformation properties to convert them into progressively converging series. These procedures involve cumbersome expressions and break down for the case of $\mathbf{k} = 0$. Direct computation gives $D_{\alpha\beta}(0; a, a, a) = 0$. Yet, in fact, the behavior in the long wavelength limit $\mathbf{k} \rightarrow 0$ is very sensitive to the way the limit is approached [11]. In general, for arbitrary lattice constants a_1 , a_2 and a_3 the result depends not only on the angle between $\boldsymbol{\mu}^P$ and \mathbf{k} but also on their own orientations with respect to the crystal axes. For the purpose of studying the dimensional crossover effect we present a simple but rigorous method for the evaluation of the dipolar interaction which displays all the above-mentioned dependences explicitly. No ambiguity arises regarding the long wavelength limit since the way $\mathbf{k} \rightarrow 0$ is precisely accounted for via the necessary angle dependence. Our method is highly suitable for the compu-

tion, gives the result to any degree of accuracy and can be extended beyond the dipolar interaction to calculate various types of forces between molecules in organic networks.

We make the following decomposition,

$$\sum_{\{n_i\}}' \equiv \sum_{n_1}' + \sum_{n_2}' \sum_{n_1} + \sum_{n_3}' \sum_{n_1 n_2}, \quad (3)$$

which comprises three kinds of contribution corresponding to the three terms in the r.h.s. of Eq. (3). The first contribution is only due to the dipoles along the chain of the x axis. The second one accounts for the interaction in the (x, y) plane except for the one among the dipoles in the x axis. The last contribution gives the result due to the remaining interaction in the whole lattice. The decomposition (3) thus means that we sum chain by chain for the plane, and plane by plane for the lattice. For $a_3 \gg a_1, a_2$ only the two first contributions survive, which is the 2D case if $a_1 = a_2$, while for $a_2, a_3 \gg a_1$ the only remaining contribution, the first one, yields the 1D limit. For arbitrary a_1, a_2, a_3 we have the dependence on the lattice-constants' ratios, which shows crossover from one to another dimension. The first contribution in Eq. (3) can exactly be evaluated without any difficulty. For the second and the third ones, we use the Fourier transforms to cast them into equivalent sums over the corresponding lattice vectors in the reciprocal space and then resort to the Parseval formula. It is worth noticing that the method of Fourier transforms was also developed in Ref. [15] to calculate lattice multipole sums for local field, polarization energy, . . . , in perfect as well as in imperfect molecular crystals. Now let $\boldsymbol{\mu}^P = (|\boldsymbol{\mu}^P|, \phi, \theta)$, $\mathbf{k} = (k, \phi', \theta')$, $\gamma_2 = a_2/a_1$ and $\gamma_3 = a_3/a_1$, where ϕ (ϕ') is the angle between the x axis and the component of $\boldsymbol{\mu}^P(\mathbf{k})$ projected on the (x, y) plane and θ (θ') that between $\boldsymbol{\mu}^P(\mathbf{k})$ and the z axis. We have obtained the most general result [17] for any possible parameters, whose particular case of the long wavelength limit reduces to

$$D^P \equiv D^{\mu^P} = \frac{|\boldsymbol{\mu}^P|^2}{a_1^3} \left(A(\gamma_2) \cos^2 \phi \sin^2 \theta + B(\gamma_2) \sin^2 \phi \sin^2 \theta + C(\gamma_2, \gamma_3) \cos^2 \theta + \frac{4\pi}{\gamma_2 \gamma_3} \cos^2 \Phi + \frac{4\pi^2}{\gamma_2} Q(\gamma_2, \gamma_3) \right), \quad (4)$$

where

$$A(\gamma_2) = -4\xi(3) + 32\pi^2 I(\gamma_2), \quad (5)$$

$$B(\gamma_2) = 2\xi(3) - 32\pi^2 I(\gamma_2) - \frac{2\pi^2}{3\gamma_2^2} - \frac{16\pi}{\gamma_2} J(\gamma_2), \quad (6)$$

$$C(\gamma_2, \gamma_3) = 2\xi(3) + \frac{2\pi^2}{3\gamma_2^2} + \frac{16\pi}{\gamma_2} J(\gamma_2) - \frac{12\pi^2}{\gamma_2} Q(\gamma_2, \gamma_3) - \frac{4\pi}{\gamma_2\gamma_3}, \quad (7)$$

with $\xi(3) = \pi^3/25.7944$ the Riemann zeta function of order three, and

$$I(\gamma_2) = \sum_{n_1=1, n_2=1}^{\infty} n_1^2 K_0(2\pi\gamma_2 n_1 n_2), \quad (8)$$

$$J(\gamma_2) = \sum_{n_1=1, n_2=1}^{\infty} \frac{n_1}{n_2} K_1(2\pi\gamma_2 n_1 n_2), \quad (9)$$

$$Q(\gamma_2, \gamma_3) = \sum'_{n_1 n_2} \frac{\sqrt{n_1^2 + n_2^2/\gamma_2^2}}{\exp(2\pi\gamma_3 \sqrt{n_1^2 + n_2^2/\gamma_2^2}) - 1}. \quad (10)$$

In Eq. (4) Φ is the angle between μ^P and k , i.e.,

$$\Phi = \arccos[\cos \theta \cos \theta' + \sin \theta \sin \theta' \cos(\phi - \phi')]. \quad (11)$$

Several remarks are in order. (i) The only quantities to be numerically computed are the I , J and Q defined by Eqs. (8) to (10). These, thanks to the presence of the modified Bessel functions of the second kind K_ν and the exponent, converge very quickly with any wanted accuracy. The obtained dependences on the relevant parameters of the system are very simple analytically as seen from Eqs. (4)–(11). (ii) The plane-wise scheme of summation of the third contribution in Eq. (3) follows that of Refs. [13,14], where, however, only the situation of $\theta = \theta' = 0$ was considered, which is a particular case of ours. For the two other contributions in Eq. (3), Refs. [13,14] introduced (also only for $\theta = \theta' = 0$) an artificial auxiliary converging factor by means of gamma and incomplete gamma functions, whereas we deal with these two contributions separately. The first one is directly summed up yielding the exact result in terms of the

Riemann zeta function $\zeta(3)$, while for the second one we sum it chain by chain. Our chain-wise scheme of summation in the reference plane is new and natural. Note that the contribution of the interaction in the reference plane is predominant over that between the reference plane and other planes. The latter contribution falls off very fast as the separation from the reference plane increases. (iii) For lattice constants different from each other, the result exhibits strong dependence on the orientation of both μ^P and k . It is known that when $a_1 = a_2 = a_3 = a$ only the angle Φ between μ^P and k plays a role. This physical fact is easily followed from our formulae. Indeed, for $a_1 = a_2 = a_3 = a$, i.e., $\gamma_2 = \gamma_3 = 1$, we have $I(1) = 9.2266 \times 10^{-4}$, $J(1) = 9.8951 \times 10^{-4}$ and $Q(1, 1) = 8.3087 \times 10^{-3}$ yielding $A(1) = B(1) = C(1, 1) = -4.5168$. Hence, in Eq. (4) all the angle dependences disappear except for the Φ -dependence and we have $a^3 D^P / |\mu^P|^2 = 8.3776$ (i.e., $\frac{8}{3}\pi$) for $\Phi = 0$ and -4.1888 (i.e., $-\frac{4}{3}\pi$) for $\Phi = \frac{1}{2}\pi$ which are the well-recognized results for 3D cubic molecular lattices [18]. For the 2D limit, when $a_3 \gg a_1 = a_2 = a$, only the θ -dependence remains and we have $a^3 D^P / |\mu^P|^2 = A(1) = -4.5168$ for $\theta = \frac{1}{2}\pi$ and $a^3 D^P / |\mu^P|^2 = C(1, \infty) = -A(1) - B(1) = 9.0336$ for $\theta = 0$. These values are in excellent agreement with those calculated in Ref. [19]. The 1D limit result ($a = a_1 \ll a_2, a_3$) is simply $a^3 D^P / |\mu^P|^2 = -4\zeta(3) = -4.8082$ and $2\zeta(3) = 2.4041$ for μ^P pointing along and perpendicularly to the x axis, respectively. The exact values obtained for the 1D, 2D and 3D limits certify the correctness of our formulae. (iv) The most important point is that our formulae, besides being simple in form, contain all the desired dependences explicitly. The γ_2 - and γ_3 -dependence will provide us with dimensional crossover diagrams, which via the angle dependences are very sensitive to concrete polarization configurations even in the long wavelength limit.

3. 1D–3D crossover

Depending on a photo-exciting beam the exciton wavevector k may have any orientation, though its absolute value is small. The pathological behavior near $k = 0$ is associated with the k -orientation in the limit $k \rightarrow 0$. It was thought that the dipolar interaction undergoes a discontinuity at $k = 0$ [11]. Such a dis-

continuity is, however, caused by an abrupt change of direction of \mathbf{k} (one often changes the \mathbf{k} -direction by $\frac{1}{2}\pi$ and observes the so-called longitudinal–transverse (L–T) splitting). In fact, if the angle dependences are described properly, as in our formulae, the physical properties change continuously as a function of the orientation of both μ^P and \mathbf{k} as well as of a_1, a_2 and a_3 . We will show this by studying the angle-dependent dimensional crossover effect. For the 1D–3D crossover, we set $a_2 = a_3$ and vary the ratio $s = a_1/a_2 = a_1/a_3$ in such a way that $0 \leq s \leq 1$. To have a closer look at the orientation dependence we consider three situations: when \mathbf{k} lies on (i) the (x, y) plane, (ii) the (x, z) plane and (iii) the (y, z) plane. For case (i), $\mathbf{k} = (k \rightarrow 0, \phi', \frac{1}{2}\pi)$, we choose $\mu^I \parallel \mathbf{k}$ (i.e., $\mu^I = (|\mu^I|, \phi = \phi', \frac{1}{2}\pi)$), $\mu^{II} \parallel z$ axis and $\mu^{III} \perp (\mu^I, \mu^{II})$. Throughout this work, for simplicity, we assume $|\mu^I| = |\mu^{II}| = |\mu^{III}| = \mu$ but we can derive the effects for the case of different $|\mu^P|$ by adjusting their magnitudes and the origin of split-off levels due to other interactions. 1D–3D crossover diagrams are represented in Fig. 1 as a function of s for several values of ϕ . For $\phi = 0$, from a viewpoint of symmetry, mode II and mode III are equivalent (here the term mode P is used as shorthand for the normalized dipolar interaction $\mu^2 D^P/a_i^3$): they cross over from 1D to 3D in the same manner. When the orientation of \mathbf{k} changes, mode II is unaffected, but mode I and mode III are influenced differently due to their polarization configurations and due to the difference in the lattice constants that they feel. Except for $\phi = \frac{1}{2}\pi$, we encounter intersections between the modes for $0 < s < 1$. Such degeneracies originate from the dimensional crossover effect and should strongly govern the optical response of the system concerned, i.e., the system which is neither of strict 1D nor 3D character. The continuous modification of the behavior of the modes in accordance with the change of direction of \mathbf{k} is visual from Fig. 2 where we plot the modes as a function of ϕ for different fixed values of s . Fig. 2a with $s = 0$ (i.e., $a_2, a_3 \gg a_1$) corresponds to the 1D limit. Relative to the x axis, mode I and mode III exchange their behavior when ϕ varies from 0 to $\frac{1}{2}\pi$. For the 3D limit ($s = 1$, i.e., $a_1 = a_2 = a_3$), Fig. 2c illustrates what was said in Section 2. There is no ϕ -dependence and the modes are determined by the angle ϕ : mode I is 3D longitudinal, whereas

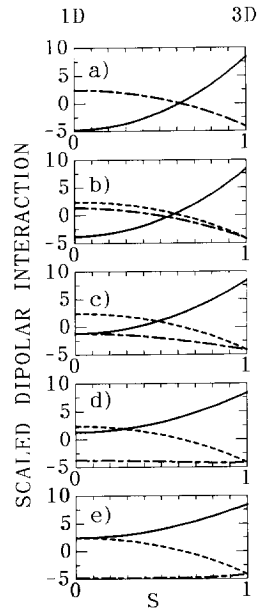


Fig. 1. Crossover between 1D and 3D of the scaled dipolar interaction $\mu^2 D^P/a_i^3$ ($P = I, II$ and III correspond to solid, dashed and dash-dotted curves, respectively; this style of identifying the curves is used for all the figures in this work) for case (i) when the lattice constant ratio $s = a_1/a_2 = a_1/a_3$ changes from 0 to 1 and (a) $\phi = 0$: mode II and mode III are coincident, (b) $\phi = \frac{1}{8}\pi$, (c) $\phi = \frac{1}{4}\pi$, (d) $\phi = \frac{3}{8}\pi$ and (e) $\phi = \frac{1}{2}\pi$.

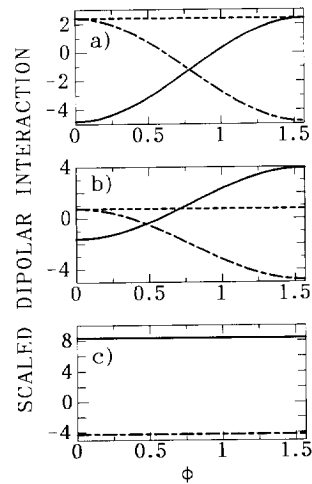


Fig. 2. Continuous modification of the modes in Fig. 1 when the direction of \mathbf{k} in the (x, y) plane changes: ϕ changes from 0 to $\frac{1}{2}\pi$ and the lattice constant ratio is fixed to (a) $s = 0$, (b) $s = 0.5$ and (c) $s = 1$: mode II and mode III are coincident.

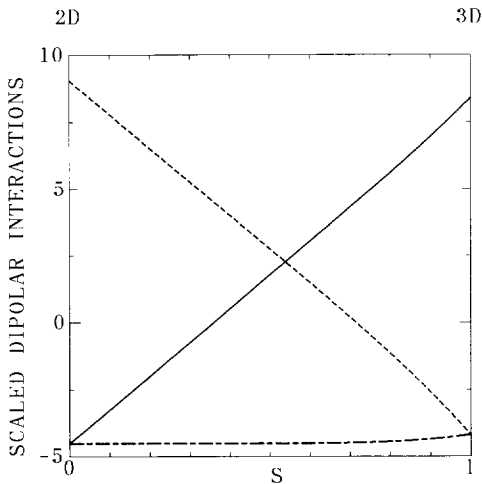


Fig. 3. 2D–3D crossover for case (i). No angle dependence. Here $s = a_1/a_3 = a_2/a_3$.

mode II and mode III are identical and behave as 3D transverse ones. Fig. 2b represents the case of $s = 0.5$.

For case (ii), $\mathbf{k} = (k \rightarrow 0, 0, \theta')$, we choose $\boldsymbol{\mu}^I \parallel \mathbf{k}$ (i.e., $\boldsymbol{\mu}^I = (|\boldsymbol{\mu}^I|, 0, \theta = \theta')$), $\boldsymbol{\mu}^{II} \parallel y$ axis and $\boldsymbol{\mu}^{III} \perp (\boldsymbol{\mu}^I, \boldsymbol{\mu}^{II})$. Due to the symmetry of the configurations under study, the 1D–3D crossover diagrams in this case for $\theta = 0, \frac{1}{8}\pi, \frac{1}{4}\pi, \frac{3}{8}\pi$ and $\frac{1}{2}\pi$ coincide with those in case (i) for $\phi = \frac{1}{2}\pi, \frac{3}{8}\pi, \frac{1}{4}\pi, \frac{1}{8}\pi$ and 0, respectively.

When \mathbf{k} lies on the (y, z) plane, $\mathbf{k} = (k \rightarrow 0, \frac{1}{2}\pi, \theta')$, we choose $\boldsymbol{\mu}^I \parallel \mathbf{k}$ (i.e., $\boldsymbol{\mu}^I = (|\boldsymbol{\mu}^I|, \frac{1}{2}\pi, \theta = \theta')$), $\boldsymbol{\mu}^{II} \parallel x$ axis and $\boldsymbol{\mu}^{III} \perp (\boldsymbol{\mu}^I, \boldsymbol{\mu}^{III})$. Then, the crossover diagram is independent of the orientation of \mathbf{k} in the (y, z) plane and it looks exactly like that in case (i) for $\phi = \frac{1}{2}\pi$ and that in case (ii) for $\theta = 0$ as is expected.

4. 2D–3D crossover

We now set $a_1 = a_2$ and define s by $s = a_1/a_3 = a_2/a_3$. For $s = 0$ (i.e., $a_3 \gg a_1 = a_2$) we have the 2D limit while the 3D limit is reached when $s = 1$ (i.e., $a_1 = a_2 = a_3$). For s varying from 0 to 1 the network crosses over from 2D to 3D. Case (i) with $\mathbf{k} = (k \rightarrow 0, \phi', \frac{1}{2}\pi)$ displays no $(\phi = \phi')$ -dependence because $a_1 = a_2$ and the corresponding 2D–3D crossover diagram is depicted in Fig. 3. Relative to the (x, y) plane, in the 2D limit, mode I and mode III are the in-plane modes but mode II is the perpendicular-to-the-plane

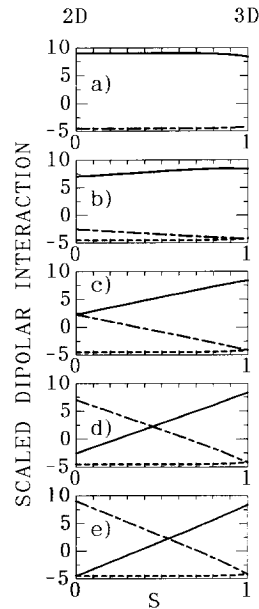


Fig. 4. Angle-dependent 2D–3D crossover as a function of $s = a_1/a_3 = a_2/a_3$ for case (ii) (and case (iii) with the modified labelling of the modes as compared to that in Section 3, see text). (a) $\theta = 0$: mode II and mode III are coincident, (b) $\theta = \frac{1}{8}\pi$, (c) $\theta = \frac{1}{4}\pi$, (d) $\theta = \frac{3}{8}\pi$ and (e) $\theta = \frac{1}{2}\pi$.

mode. That is why for $s = 0$ mode I and mode III are degenerate but mode II is split off. When s increases to 1, the network becomes of 3D character, mode I becomes a longitudinal mode in the 3D limit, whereas mode II and mode III become transverse ones. That explains why mode I and mode II intersect during crossing over from 2D to 3D. This modes' intersection is again due to the dimensional crossover effect and should bring about certain consequences in the optical response of the network with unequal lattice constants.

For case (ii) the polarization configuration is chosen similar to that in Section 3. Nevertheless, for case (iii) here we choose $\boldsymbol{\mu}^I \parallel \mathbf{k}$, $\boldsymbol{\mu}^{II} \parallel x$ axis (not $\boldsymbol{\mu}^{III}$ as in Section 3) and $\boldsymbol{\mu}^{III} \perp (\boldsymbol{\mu}^I, \boldsymbol{\mu}^{II})$. Then, the θ -dependent 2D–3D crossover diagrams for case (ii) and case (iii) are the same that are drawn in Fig. 4. Note that Figs. 4e and 3 are physically identical besides exchange of modes II and III by definition.

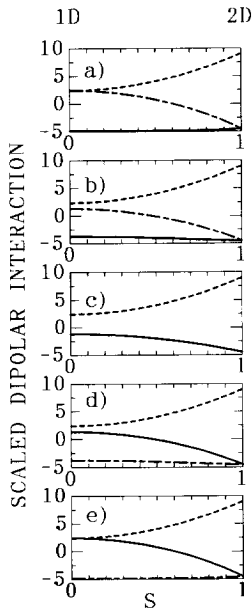


Fig. 5. Angle-dependent 1D–2D crossover as a function of $s = a_1/a_2$ in the (x, y) plane for (a) $\phi = 0$, (b) $\phi = \frac{1}{8}\pi$, (c) $\phi = \frac{1}{4}\pi$: mode I and mode III are coincident, (d) $\phi = \frac{3}{8}\pi$: mode I (mode III) behaves like mode III (mode I) when $\phi = \frac{1}{8}\pi$, and (e) $\phi = \frac{1}{2}\pi$: mode I (mode III) behaves like mode III (mode I) when $\phi = 0$.

5. 1D–2D crossover

When $a_3 \gg a_1, a_2$ the propagation of the exciton along the direction perpendicular to the (x, y) plane is negligible. Furthermore, in the long wavelength limit the dipolar interaction in the (x, y) plane is not sensitive to the way $\mathbf{k} \rightarrow 0$. In this limit it depends only on the orientation of the vectors $\boldsymbol{\mu}^P$. This property is justified from our Eq. (4), which for $a_3 \gg a_1, a_2$ simplifies to

$$D^P = \frac{|\boldsymbol{\mu}^P|^2}{a_1^3} [A(\gamma_2)(\cos^2 \phi \sin^2 \theta - \cos^2 \theta) + B(\gamma_2)(\sin^2 \phi \sin^2 \theta - \cos^2 \theta)]. \quad (12)$$

If we choose $\boldsymbol{\mu}^I = (|\boldsymbol{\mu}^I|, \phi, \frac{1}{2}\pi) \parallel \mathbf{k}$, $\boldsymbol{\mu}^{II} \parallel z$ axis and $\boldsymbol{\mu}^{III} \perp (\boldsymbol{\mu}^I, \boldsymbol{\mu}^{II})$, then only the ϕ -dependence remains. In Fig. 5 we plot the 1D–2D crossover as a function of $s = 1/\gamma_2 = a_1/a_2$ for different values of ϕ . Due to its orientation, which is perpendicular to the 2D plane, mode II crosses over from 1D to 2D inde-

pendent of ϕ . Since both $\boldsymbol{\mu}^I$ and $\boldsymbol{\mu}^{III}$ lie on the (x, y) plane and for $\phi = \frac{1}{4}\pi$ they have the same orientation relative to the x direction, mode I and mode III are identical in crossing over from 1D to 2D (see Fig. 5c for $\phi = \frac{1}{4}\pi$). Further, these two modes, mode I and mode III, exchange their behavior under the situation when $\phi = \phi_0$ and $\phi = \frac{1}{2}\pi - \phi_0$ (ϕ_0 any angle): compare, e.g., Fig. 5a with Fig. 5e and Fig. 5b with Fig. 5d.

6. Discussion and conclusion

We have worked out analytical formulae for the evaluation of the exciton dipolar interaction in an organic network of any dimension. Our formulae use no approximations and are very useful for the numerical computation. Also, they could serve as a possible guide towards producing a material of desired dimension and properties. All dependences on the orientation of $\boldsymbol{\mu}^P$ and \mathbf{k} as well as on arbitrary lattice constants a_1, a_2 and a_3 are taken into account explicitly. This allows us not only to calculate the dipolar interaction for a given set of the parameters but also to study the angle-dependent dimensional crossover effect. As shown in the text, there is no ambiguity in the evaluation regarding the way $\mathbf{k} \rightarrow 0$ even in the long wavelength limit: the result is a continuous function of all the parameters involved. To the best of our knowledge, such convenient expressions have not been available though the dipolar interaction was evaluated by many authors. Note that decomposition (3) is not unique. We made it just for the purpose of studying the dimensional crossover effect with the x axis and the (x, y) plane as the reference direction and reference plane. With other wanted reference directions and planes, alternative decompositions can be done by an appropriate permutation among n_1, n_2 and n_3 in (3). However, not all decompositions are reasonable. Since the interaction decreases against distance, the recipe is that for $a_\alpha \leq a_\beta \leq a_\gamma$ (α, β, γ are 1, 2 or 3, but not equal to each other) the appropriate decomposition must be as $\sum'_{\{n_i\}} \equiv \sum'_{n_\alpha} + \sum'_{n_\beta} \sum_{n_\alpha} + \sum'_{n_\gamma} \sum_{n_\alpha n_\beta}$. In this sense, decomposition (3) and our formulae are applicable to the case of $a_1 \leq a_2 \leq a_3$, for which the studied dimensional crossovers are meaningful.

We now briefly discuss the expected consequences related to the optical response of the organic network.

The lattice constants of organic networks are of the order of 1 Å and several tens of Å, which is much shorter than the wavelength λ of the relevant radiation field (λ is several thousands of Å). Therefore, one is able to observe the crossover effect by optical responses of the network. Note also that the electronic transition dipole moments are always 3D vectors although the excitation propagation may be limited to a reduced dimension. As a matter of fact, the optical response is much governed by the level splitting and degeneracy at and near $k = 0$. For strict 1D ($a_1 \ll a_2, a_3$), 2D ($a_1 = a_2 \ll a_3$) and 3D ($a_1 = a_2 = a_3$) the exciton wavevector along the x axis, in the (x, y) plane and in the bulk, respectively, is a good quantum number. Then one can speak of the single longitudinal and doubly degenerate transverse modes and there arises the well-known L–T splitting in the long wavelength limit. In 3D materials only the T mode is optically active and the radiation is almost totally reflected in the frequency region between the L mode and the T mode. In 1D and 2D materials the reflection spectra are more complicated because both the T mode and the L mode can be coupled to the light and we have mixed modes of the coupled light–matter system. In general, things change qualitatively when we deal with organic networks with different lattice constants in the three directions. As illustrated in the figures, the level splitting is too sensitive to both the lattice constant ratios and the orientation of μ^P and k . Take, for instance, Figs. 1a and 1e. The corresponding 1D–3D crossover is completely distinct for $\phi = 0$ and $\phi = \frac{1}{2}\pi$. In Fig. 1a (1e) the network crosses over with (without) an intersection between modes when $0 < s < 1$. In Fig. 1a at $s = s_0 \simeq 0.615$ the three modes suffer an interesting degeneracy due to the dimensional crossover effect resulting in no level splitting as it is for $s \neq s_0$. In Fig. 1e, on the other hand, the three modes are always split off for $0 < s < 1$, whereas in the 1D (3D) limit mode II is degenerate with mode I (mode III). Similar features also happen in Fig. 3, Figs. 4d, 4e, Figs. 4b, 4c and also Fig. 2. Furthermore, under the same angle, mode intersections occur only at certain values of the lattice constant ratio (see Figs. 1a–1d, Fig. 3 and Figs. 4d, 4e). In view of all this, networks with even slightly unequal lattice constants may have quite different level splittings and thus response to the light in quite different manners. Calculation of optical properties of different types of organic networks

with direction dependences adequately taken into account is therefore a hard task. However, we could expect the partial transparency due to the mixed modes for frequencies between the L and T modes of 1D systems, e.g., at $s = 0$ in Fig. 1a and the singularity enhanced reflections around these two frequencies at $s = 0$. These two singularities collapse into a single one around $s = s_0$ and the total reflection would be recovered for $s = 1$, i.e., a 3D system. Since we have obtained the most general result [17], we know also the exciton dispersion in any strict dimension as well as in the case when the network cannot be said to be of a certain strict dimension because of the difference in its lattice constants. We do hope that with the help of such general formulae with all the necessary dependences being included explicitly, we will be able to investigate in the near future the optical response of various organic networks under some concrete pump, propagation and polarization configurations which are realizable experimentally. Level splittings could be tailor-made for a possible practical application by changing the lattice constants and adjusting the experimental configuration.

Acknowledgement

The authors are grateful to Professors V.M. Agranovich and K. Miyano for stimulating and valuable discussions. This work is jointly supported by the Japan Society for the Promotion of Science (JSPS) and by a Grant-in-Aid for Scientific Research on the Priority Area “Mutual and Quantum Control of Radiation and Electronic Systems” from the Ministry of Education, Science and Culture of Japan.

References

- [1] A. Nabetani, A. Tomioka, H. Tamaru and K. Miyano, submitted to J. Chem. Phys.
- [2] F.F. So, S.R. Forrest, Y.Q. Shi and W.H. Steier, Appl. Phys. Lett. 56 (1990) 674; F.F. So and S.R. Forrest, Phys. Rev. Lett. 66 (1991) 2649.
- [3] T. Nonaka, T. Date, S. Tomita, N. Nagai, M. Nishimura, Y. Murata and A. Ishitani, Thin Solid Films 237 (1994) 87; T. Nonaka, Y. Mori, N. Nagai, Y. Nakagawa, N. Saeda, T. Takahagi and A. Ishitani, Thin Solid Films 239 (1994) 214.
- [4] V.M. Agranovich, Mol. Cryst. Liq. Cryst. 230 (1993) 13.
- [5] M. Kuwata-Gonokami, N. Peyghambarian, K. Meissner, B. Fluegel, Y. Sato, K. Ema, R. Shimano, S. Mazumdar, F.

- Guo, T. Tokihiro, H. Ezaki and E. Hanamura, *Nature* 367 (1994) 47.
- [6] M. Hirasawa, T. Ishihara and T. Goto, *J. Phys. Soc. Japan* 63 (1994) 3870.
- [7] V.M. Agranovich and A.M. Kamchatnov, *JETP Lett.* 59 (1994) 397.
- [8] V. Agranovich, R. Atanasov and F. Bassani, *Solid State Commun.* 92 (1994) 295.
- [9] P.P. Ewald, *Ann. Phys. (Leipzig)* 64 (1921) 253.
- [10] M. Born and M. Bradburn, *Proc. Cambridge Philos. Soc.* 39 (1943) 104.
- [11] M.H. Cohen and F. Keffer, *Phys. Rev.* 99 (1955) 1128.
- [12] B.R.A. Nijboer and F.W. De Wette, *Physica* XXIII (1957) 309.
- [13] B.R.A. Nijboer and F.W. De Wette, *Physica* XXIV (1958) 422.
- [14] M.R. Philpott, *J. Chem. Phys.* 58 (1973) 588.
- [15] P.J. Bounds and R.W. Munn, *Chem. Phys.* 44 (1979) 103; 59 (1981) 47.
- [16] K. Fuchizaki, *J. Phys. Soc. Japan* 63 (1994) 4051.
- [17] Nguyen Ba An and E. Hanamura, unpublished.
- [18] W.R. Heller and A. Marcus, *Phys. Rev.* 84 (1951) 44.
- [19] B.M.E. Van der Hoff and G.C. Benson, *Can. J. Phys.* 31 (1953) 1087.